Efficient Numerical Simulation of the Time Dependence of Electronic Energy Transfer in Polymers. 3. Depolarization, Förster Transfer, and Trapping

Jeffrey D. Byers, W. Samuel Parsons, and S. E. Webber*

Department of Chemistry and Biochemistry and Center for Polymer Research, The University of Texas at Austin, Austin, Texas 78712

Received March 16, 1992; Revised Manuscript Received July 8, 1992

ABSTRACT: Statistical ensembles of polymer configurations have been generated using the pivot algorithm with interaction energy for the calculation of the time dependence of the survival probability of a donor excited state in the presence of down-chain Förster dipole–dipole transfer between polymer chromophores with simultaneous Förster trapping and of the depolarization without trapping. Five methods of placing traps on the polymer coil have been investigated, with a discussion of the applicability of the various methods to the observed behavior of the fluorescence decay.

Introduction

A great deal of research has been devoted to specific models and/or geometries dealing with the numerical simulation of electronic energy transfer (EET), or excitation transport, on polymer coils in condensed media with the goal of determining polymer conformation and morphology.[1-5] Our previous calculations were applied to self-avoiding polymer coils embedded in a cubic lattice with pendant chromophores occupying lattice sites and having randomly placed disruptive traps.[3,4] Until recently, these calculations were carried out for simulated polymer coils having short-range (nearest-neighbor) transfer between chromophores with trapping by the Förster dipole–dipole mechanism.[6] The present paper extends this work to consider migration of the excitation via the Förster mechanism.

The calculation of statistical ensembles of polymer coils requires the generation of large numbers of polymer configurations (on the order of 10^6 for length 100). To achieve this requirement, we have utilized a variation of the pivot algorithm which includes interaction energy, as developed by Johnson et al.[7] We find that this method is capable of generating statistically distinct configurations with the accompanying thermodynamic calculations 5–10 times faster than the equivalent calculation using a standard static Monte Carlo self-avoiding walk technique employed by us in the past. Combined with increased computation capabilities, this has allowed us to generate ensembles with 50–100 times the number of configurations of our previous calculations,[8] thus improving the statistics of these calculations.

Our simulations also lend themselves to the calculation of fluorescence depolarization via EET for polymer coils with a low chromophore loading. This enables us to compare the depolarization from donor–donor excited-state transport with that calculated by Fayer and coworkers[5] and subsequently to calculate the fluorescence decay for polymer coils having a low loading of chromophores.

In an attempt to improve the polymer model, we have introduced two new sets of calculations. First, we expended the allowed chromophore–chromophore transfer distance to 3 lattice units rather than simple nearest-neighbor transfer. The significance of limiting the transfer distance to 3 lattice units will be discussed later. Second, we place the disruptive traps on the polymer in a more realistic manner than the simple random placement used previously and examine the effect of different trap placement schemes on the excited-state survival probability.

We hope to demonstrate that this method of polymer modeling is useful in elucidating at least the qualitative trends in EET and depolarization for polymer coils, thus helping us understand the factors involved in determining the experimentally observed behavior. As well be discussed later, the agreement between calculated and experimental data is quantitative in the latter case.

Polymer Model

The simulated polymer configurations in our calculations are randomly generated self-avoiding polymer coils embedded in a three-dimensional cubic lattice. At present, the lattice is a necessary restriction of the model since there is not a method available to use for the efficient generation of the large number of off-lattice polymer coils required for a statistical sampling. The pendant chromophores are assumed to occupy lattice sites and are dimensionless. We emply a single parameter to describe the interaction strength between the solvent and the polymer, the intersegmental interaction energy parameter, $\phi = -\epsilon/kT$. ϵ is the intersegmental contact energy for nonbonded nearest neighbors, and we vary the interaction parameter from $\phi = 0.0$ to $\phi = 0.35$. The average coil is expanded and has relatively few nonbonded nearest-neighbor contacts at $\phi = 0.0$, which corresponds to a good solvent environment. At $\phi = 0.35$, the average polymer is collapsed, which corresponds to a poor solvent environment. In the case of EET on polymer coils with traps, the traps are placed on lattice sites and considered to be infintely deep potential wells which instantly quench any excitation which "hops" to a trap site (i.e., disruptive traps). The depolarization calculations were carried out at different ϕ values including the Flory Θ-point ($\phi = 0.275$) which corresponds to a polymer in a solid solution. For these latter calculations chromophore concentrations on the polymer coil were chosen to be identical to those experimental results provided to us for comparison by Fayer.[9]

Pivot Algorithm

Each polymer configuration was generated using the pivot algorithm with an interaction energy, where the ensemble for the chosen interaction parameter was constructed by using the Metropolis method of energy

0024-9297/92/2225-5935$03.00/0

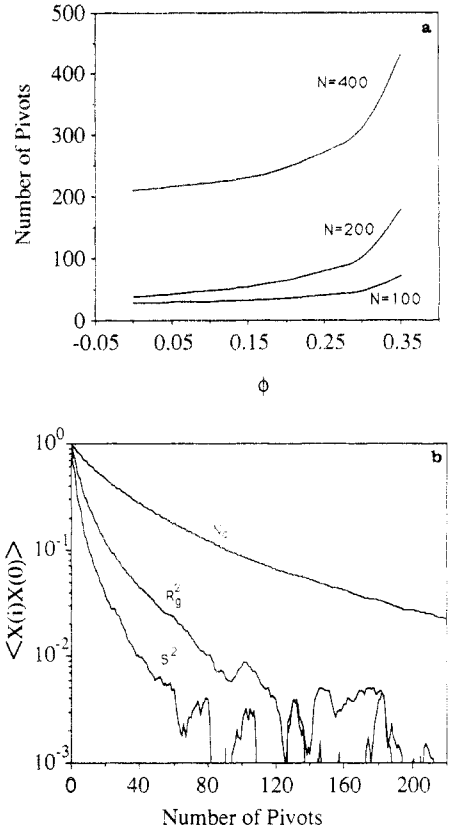

Figure 1. (a) Autocorrelation lifetime for contacts as a function of ϕ. (b) Autocorrelation function for N_c, R_g^2 and S^2 (N = 100, ϕ = 0.0).

sampling.[7] The pivot algorithm is a dynamic Monte Carlo technique that generates polymer configurations approximately 1 order of N faster than standard static Monte Carlo generation methods, where N is the length of the polymer coil being generated. This method allows the generation of statistical ensembles of polymer coils for lengths longer than was previously practical. (At present, even using the pivot algorithm, it is impractical for N to exceed 6400.[10]) The algorithm begins with an initial polymer configuration which has been "thermalized" both to remove the initialization bias and to generate a configuration at equilibrium in the chosen interaction parameter distribution. The number of iterations required to generate an equilibrium configuration is dependent on the initial configuration (we use a straight chain for simplicity) and on the desired interaction parameter. This is determined by the autocorrelation lifetime of the algorithm for each set of parameters, where the autocorrelation function is given by[10]

$$\langle X(i)\, X(0)\rangle = \frac{\sum_{j=1}^{N-i} X_j X_{j-i}}{N-i} - \left[\frac{\sum_{j=1}^{N} X_j}{N}\right]^2 \qquad (1)$$

Mandras and Sokal have demonstrated that 10 autocorrelation lifetimes are sufficient to assure that the initialization bias has been removed, given a straight chain as the initial configuration.[10] Each new configuration is generated by performing a random operation from the octahedral point group on the section of the polymer coil from the pivot point (a randomly chosen lattice site on the polymer coil) to end of the chain of the previous polymer configuration. If this new coil both is self-avoiding and passes the Metropolis test for energy, it is accepted.

Since two consecutive accepted configurations are significantly correlated (it is possible for the two polymer coils to be identical in consecutive configurations), the configurations included in a calculated ensemble should be chosen from the accepted configurations at intervals such that they are sufficiently different as to be distinct and essentially uncorrelated. The autocorrelation lifetimes, τ, were measured for various system variables for all ensembles generated by making the assumption that the autocorrelation function can be adequately approximated by a single exponential, i.e., $\langle X(i)\, X(0)\rangle \sim e^{i/\tau_x}$ (see Bishop et al.[11] for a more detailed discussion of the autocorrelation function). This approximation is valid for a small number of pivots. The correlation time increases with the polymer length and ϕ (see Figure 1a). The pivot algorithm changes global variables (e.g., end-to-end distance) more drastically than local variables (e.g., segmental contacts) with each successive iteration. Since the Metropolis acceptance criterion directly depends on the number of nearest-neighbor contacts, the resulting autocorrelation lifetime is longer for the number of contacts than that for $\langle R_g^2\rangle$ and $\langle S^2\rangle$ (Figure 1b). This observation is important to our calculations, since the rate of energy transfer across a polymer chain is strongly influenced by the number of nonbonded nearest-neighbor contacts. To assure that successive configurations were uncorrelated, we accepted configurations into the emsemble every two lifetimes of the autocorrelation function of the number of contacts. The quantities of interest were calculated for individual polymer coils and averaged over the entire ensemble, where the number of accepted configurations per ensemble ranged from 2×10^4 to 3×10^6. The energy, E, of each polymer configuration is directly dependent on N_c, the number of nonbonded nearest-neighbor contacts: $E = \phi N_c kT$.

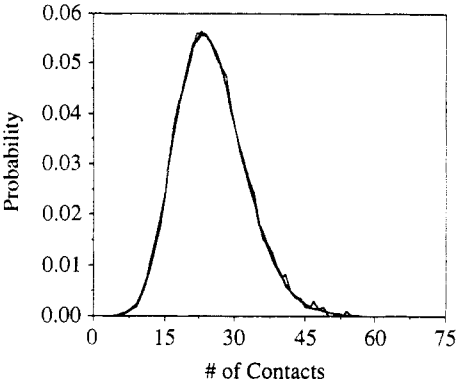

Figure 2. Comparison of true contact distribution function at ϕ = 0.15 with those obtained by transforming the distribution functions from ϕ = 0.0 and 0.275 to ϕ = 0.15 using eq 2.

If the statistics of the ensemble are good for all possible intracoil contacts, then it is straightforward to note that, given the probability of occurrence, $g(c_i)$, of a particular polymer coil having a given number of nonbonded nearest-neighbor contacts, the probability of that configuration at a different interaction energy, $g(c_i)'$, can be derived directly from the corresponding Boltzmann factors by the equation

$$g(c_i)' = g(c_i)\, \exp[c_i(\phi'-\phi)] \qquad (2)$$

In Figure 2, the approximate contact distributions for an interaction energy parameter of ϕ = 0.275 calculated from the exact distributions at ϕ' of 0.15 and 0.35 using eq 2 are compared with the exact contact distribution generated from an ensemble of the same length at ϕ = 0.275. The agreement is almost exact, which demonstrates that the pivot algorithm samples all possible contacts very efficiently. Thus eq 2 allows the transformation between

distributions to within the observed error of the ensemble. As would be expected, this method of interpolation works best for ϕ values which are close to each other and becomes progressively more inaccurate as the two ϕ values diverge. This effect is due to the degree of overlap of the contact distributions at the separate ϕ values and can only be improved upon by better statistics in the polymer ensembles.

The Metropolis method is well documented and integral to the method of polymer generation devised by Johnson et al.[7] It is discussed in detail there with respect to this method of polymer generation. Because we are using this method without notable changes in the code, we will not discuss it in detail.

Summary of the Method of Computing Time-Dependent Excitation Transport

The theory has been presented in detail in previous publications,[3,4,12] such that only a brief outline of the major results will be included here. A Pauli Master equation is used to describe the time-dependent probability that a particular chromophore is excited:

$$d\mathbf{P}(t)/dt = \mathbf{W}\mathbf{P}(t) \tag{3}$$

where the ith element of $\mathbf{P}(t)$ is the probability that the ith chromophore is excited at time t, and $\mathbf{W}$ is the transfer rate matrix, which has the dimensionality of the number of chromophores on the polymer coil. The formal solution of eq 3 is

$$\mathbf{P}(t) = \exp(\mathbf{W}t)\,\mathbf{P}(t=0) = \mathbf{G}(t)\,\mathbf{P}(t=0) \tag{4}$$

where $\mathbf{G}(t)$ represents the Green's function solution of eq 3. Since the initial probability distribution of the excitation is assumed to be uniform ($P_i(0) = 1/N$ where N is the number of chromophores), the probability that the ith chromophore will be excited at time t is

$$P_i(t) = \sum_{j=1}^{N} G_{ij}(t)\,P_j(0) = \frac{1}{N}\sum_{j=1}^{N} G_{ij}(t) \tag{5}$$

where $G_{ij}(t)$ are the elements of the Green's function solution of the Master equation.

The probability that the initially excited chromophore is excited at time t ($P_1(t)$) is of direct physical importance and corresponds to the fluorescence depolarization due to EET even if there are no traps present on the polymer coil. This value is measured experimentally using time-resolved fluorescence aniostropy and is equivalent to the value $G^s(t)$ calcualted by Fayer and co-workers.[5] $P_1(t)$ is derived from eq 4 above by noting that only diagonal elements of the solution have a nonzero contribution:

$$P_1(t) = \frac{1}{N}\langle f|\mathbf{G}(t)|f\rangle = \frac{1}{N}\langle f|\exp(\mathbf{W}t)|f\rangle \tag{6}$$

where $|f\rangle$ is a unit vector. Inserting a complete set of $\mathbf{W}$'s eigenstates, $P_1(t)$ becomes

$$P_1(t) = \frac{1}{N}\sum_{i=1}^{N}|\langle f|\lambda_i\rangle|^2 e^{\lambda_i t} = \frac{1}{N}\sum_{i=1}^{N} R_{ff}^{i} e^{\lambda_i t} \tag{7}$$

where $R_{ff}^{(i)}$ is the residue of the eignevalue λ_i of $\mathbf{W}$.[12-14] Because $|f\rangle$ is a unit vector, all of the residues are equal to 1, and eq 7 simplifies to

$$P_1(t) = \frac{1}{N}\sum_{j=1}^{N} e^{\lambda_j t} \tag{8}$$

An alternative physical observable is the fluorescence decay of the energy donor via trapping of the excitation (in this paper we consider only the Förster mechanism[6]). This is described by the total time-dependent survival probability:[3,4]

$$S(t) = \sum_{i=1}^{N} P_i(t) = \frac{1}{N}\sum_{i=1}^{N} R_{ff}^{(i)} \exp(\lambda_i t) \tag{9}$$

When the intrinsic chromophore lifetime (τ_0) is known, $S(t)$ can be derived from the fluorescence decay of the system:

$$I_{fl}(t) = e^{-t/\tau_0} S(t) \tag{10}$$

$I_{fl}(t)$ is directly measurable and can be calculated for any chromophore concentration using our method.

The elements of $\mathbf{W}$ are constructed from the chromophore separations on each polymer coil and thus must be calculated for each new configuration:

$$W_{ij} = \omega(R_{ij}) = \frac{1}{\tau}\left(\frac{R_0^{(c)}}{R_{ij}}\right) \tag{11a}$$

$$W_{ij} = -\frac{1}{\tau}\left[\sum_{j,j\neq i}\left(\frac{R_0^{(c)}}{R_{ij}}\right)^6 + \sum_{k}\left(\frac{R_0^{(t)}}{R_{jk}}\right)^6\right] \tag{11b}$$

where $R_0^{(c)}$ is the Förster radius for chromophore to chromophore transfer, $R_0^{(t)}$ is the Förster radius for chromophore to trap transfer, and k is the index of the traps on the polymer chain. In the past, a critical component in the calculation of the eigenvalues of $\mathbf{W}$ has been the use of the Lanczos algorithm,[3,4] which is especially useful for large sparse matrices. When including transfer between chromophores by the Förster mechanism, a polymer coil with a high chromophore loading would seem to preclude the use of the Lanczos algorithm for the calculation of the eigenvalues and residues, because the rate matrix for such coils would include a nonzero transfer term for every matrix element, thus generating a nonsparse matrix. With a full matrix, the Lanczos algorithm is slower than standard methods for diagonalizing matrices. However, by adopting a cutoff criterion for EET it is possible to retain the Lanczos algorithm with little loss of speed or accuracy, as will be discussed in the Results section.

In depolarization calculations a low chromophore loading leads to a rate matrix with a small dimensionality. In these cases, the transfer rate matrix cannot be truncated with acceptable results and the Lanczos algorithm therefore provides no computational advantage. This does not present a problem because the matrices are small in size and the eigenvalues were easily calculated by using a standard Householder reduction to a tridiagonal form followed by application of the QL algorithm with Wilkinson shift.[15] Since this gives an exact solution (to within roundoff error) to the master equation, the resulting curves will be accurate to within the scope of the theory behind the model.

Results

(1) Effect of Transfer to Non-Nearest Neighbors. In considering only nearest-neighbor transfer in the original model, we realized that our calculations were neglecting a potentially large contribution to the total transfer probability. This was a necessary restriction because of computational limitations which have since been removed. We therefore decided to redress this shortcoming by implementing a revised model which included essentially all of the transfer probability while preserving the numerical advantages of the Lanczos

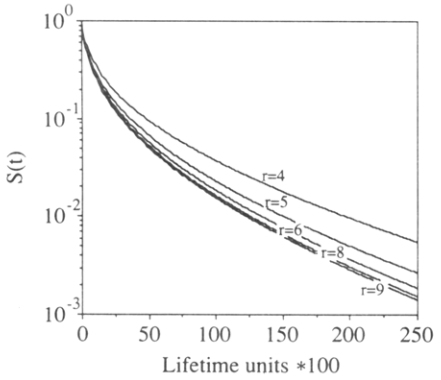

Figure 3. Survival probability for a polymer coil with $N = 100$ and $\phi = 0.275$, as a function of the allowed transfer distance when r equals the lattice units squared of the cutoff distance.

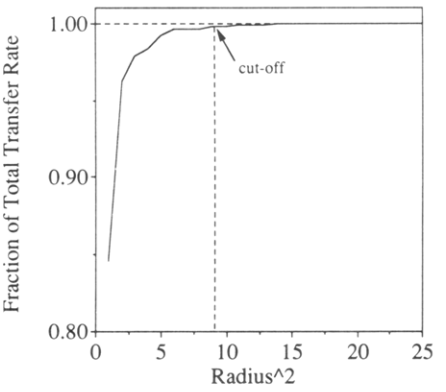

Figure 4. Plot of the transfer rate vs squared distance in lattice units ($N = 50$, $\phi = 0.0$).

Chart I

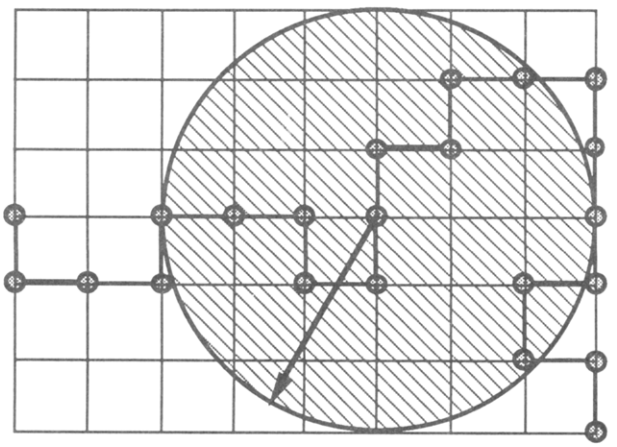

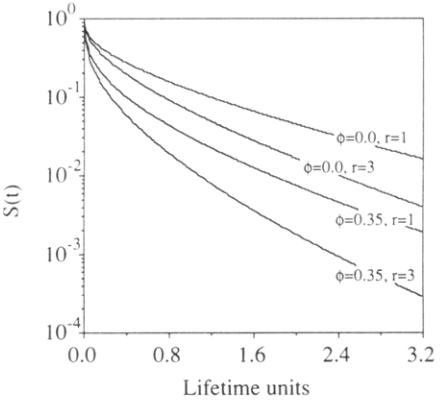

Figure 5. Survival probability for nearest-neighbor transfer ($r = 1$ lattice unit) vs Förster transfer ($r = 3$ lattice units), at the indicated ϕ value and $p = 0.005$.

solution. To achieve this, we calculated a series of survival probabilities for an identical polymer ensemble with an increasing distance of allowed chromophore–chromophore transfer (see Chart I and Figure 3). These decay curves tend to converge near a cutoff distance of 3 lattice units. Note that the value of $R_0^{(c)}$ is not important because it only provides a scaling factor for the overall rate of decay. We also calculated the integral of the transfer rate over the full polymer coil to determine when the chromophore–chromophore transfer distance cutoff was large enough to encompass approximately 99% of the total transfer rate. This cutoff distance did not depend strongly on ϕ and is independent of the magnitude of $R_0^{(c)}$ because the survival probability is directly dependent on the pairwise radial distribution function $g(r)$, where $g(r) = 4\pi r^2 r(r)$ and $r(r)$ is the density of lattice points.[4] The fraction of the total transfer rate within a sphere with a m lattice site radius is therefore

$$\frac{\int_0^m dr\, g(r)\, \omega(r)}{\int_0^\infty dr\, g(r)\, \omega(r)} \tag{12}$$

where $\omega(r)$ is given in eq 11a. Since $R_0^{(c)}$ factors out, this quantity is also independent of $R_0^{(c)}$. Because of the cubic lattice used, the different cutoff values correspond to integral values of R^2. With a polymer length of 50, a cutoff distance of 3 lattice sites was found to encompass ~99% of the total transfer rate (see Figure 4).

Limiting the allowed chromophore–chromophore transfer distance to 3 lattice units instead of the length of the polymer still neglects approximately 1% of the total transfer rate but allows the continued efficient use of the Lanczos algorithm. (This is similar to the error in the ensemble average.) We now incorporate this cutoff procedure as standard in our model, with the realization that the actual decay of the survival probability will always occur slightly faster since some transfer probability is neglected.

(2) Effect of Non-Nearest-Neighbor EET on Trapping Rate. The calculation of EET on polymer coils included Förster type transfer between chromophores with simultaneous Förster trapping, with $R_0^{(c)} = R_0^{(t)}$ for simplicity. Qualitatively, the $S(t)$ derived here have the same dependence on ϕ, polymer length (N), and trap density (p) as obtained earlier for nearest-neighbor chromophore–chromophore transfer.[4] This indicates that the qualitative results obtained from nearest-neighbor transfer are useful in describing some of the conformational relationships between EET and ϕ, N, and p but also demonstrates that nearest-neighbor transfer neglects significant transfer probability. As can be seen (Figure 5), the survival probability decays faster than when only nearest-neighbor transfer is considered. This is expected intuitively, as each excited chromophore has a greater probability of undergoing EET due to the enlarged transfer radii between chromophores.

(3) Effect of Trap Placement. In an attempt to determine the effect of trap placement on the survival probability, five different methods of placing traps on the polymer coils were investigated: (1) A fixed number of traps were randomly placed on the polymer coil. This would be appropriate for a nonperturbing covalently bound trap. The following methods were chosen to model "excimer-forming sites". (2) A fixed number of traps were placed randomly on those chromophore sites which have nonbonded nearest-neighbor contacts. (3) The number

Table I
Fraction of Trap-Free Coils for Different Trap Placement Methods[a]

		fraction of trap-free polymers		
method[b]	ϕ	$p = 0.005$	$p = 0.010$	$p = 0.015$
3	0.0	0.028	0.0002	0.0
3	0.15	0.032	0.0002	0.0
3	0.275	0.036	0.0	0.0
3	0.35	0.032	0.0002	0.0
4	0.0	0.028	0.0002	0.0
4	0.15	0.032	0.0002	0.0
4	0.275	0.036	0.0	0.0
4	0.35	0.032	0.0002	0.0
5	0.0	0.356	0.114	0.032
5	0.15	0.359	0.121	0.037
5	0.275	0.361	0.126	0.041
5	0.35	0.363	0.130	0.043

[a] For a polymer ensemble with $N = 200$. [b] See text for method of placing traps.

of traps that are randomly placed on the polymer is proportional to the number of nonbonded nearest-neighbor contacts for that individual polymer but with the requirement that the average number of traps for the ensemble is constant. (4) This method is identical to 3 above with the additional requirement that traps be placed on sites having nonbonded nearest-neighbor contacts. Thus excimer-forming sites are preferentially produced in collapsed sections of the polymer. (5) This method is an elaboration of method 4. We define a factor (f) based on the number of nonbonded nearest-neighbor contacts and the average number of traps for the ensemble, $f = \langle T \rangle / N_c$ where $\langle T \rangle$ is the average number of traps for the polymer ensemble and N_c is the number of nonbonded nearest-neighbor contacts for a particular polymer. Each nonbonded nearest-neighbor contact is individually tested to determine if it is a trap by generating a random number from 0 to $\langle T \rangle$ for each contact, comparing it to f and designating it a trap if the random number is smaller than f. Methods 3–5 allow the number of traps per coil to vary and some coils are trap-free. The number of polymer coils having no traps are counted so that the corresponding contribution to the survival probability can be added into the ensemble average. This effectively adds a constant term to the survival probability which could be used to help fit the p parameter to experimental data. As can be seen from Table I, there are a significant number of trap-free coils for ensembles having both a low trap density and a high ϕ value, and the number of trap-free coils tends to increase with ϕ. This effect is a result of the assumption that p is constant. There are a greater number of nonbonded nearest-neighbor contacts at higher ϕ, thus leading to a lower probability that any given chromophore has a trap. In considering a real polymer one would expect p to increase as the coild collapsed.

These latter methods more realistically simulate excimer trapping of excitation. When the survival probability curves are compared for the various methods (cf. Figure 6a,b), the methods which placed traps preferentially on contact sites exhibited a faster rate of decay at short times for all ϕ values and trap placements. This is expected intuitively, since the traps on contact sites in general have a greater number of chromophores that are nearby and therefore trap the excitation probability more quickly.

The long-time behavior of these calculations as a function of ϕ and trap density is quite interesting. At low ϕ values and low trap concentration, separate, noncrossing survival probabilities that appear parallel at long times are computed (e.g., see Figure 6a). At high ϕ values, and higher trap concentrations, e.g., Figure 6b, the $S(t)$ curves

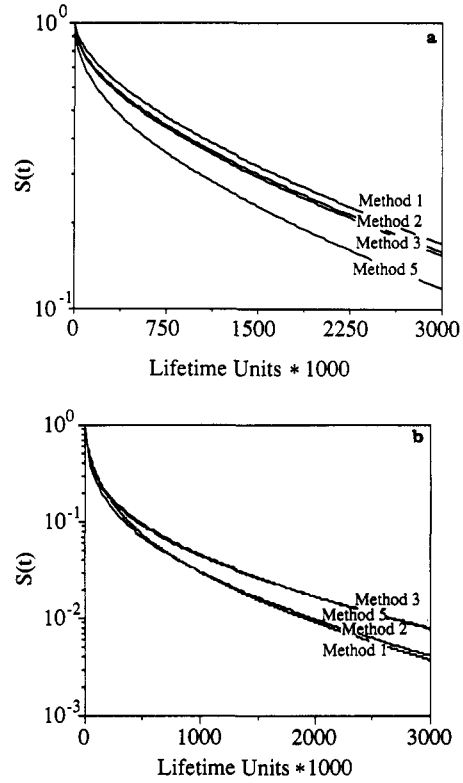

Figure 6. (a) Survival probability of different methods of trap placement for a polymer coil with $N = 200$, $\phi = 0.0$, and 1 trap per coil average. (b) Survival probability of different methods of trap placement for a polymer coil with $N = 200$, $\phi = 0.35$, and 3 traps per coil average. (Note the change in the $S(t)$ scale.)

are nearly indistinct at short times, but at later times they cross and do not appear to become parallel at long times. We note that no method produces uniformly faster decay. At low ϕ and trap densities, method 5 yields the fastest overall decay, while at high ϕ and trap densities, method 1 is fastest on the observed time scale. Method 4 produced survival probability curves which did not deviate noticeably at any of the calculated parameter values from method 3, and consequently the corresponding curves are not presented.

(4) Interpolation of $S(t)$ Curves from Different Trap Densities. The survival probability for a polymer ensemble can be interpolated from a calculated survival probability curve with a different trap density but which otherise has identical parameters. This interpolation is linear in log $S(t)$ space for low trap concentration, i.e., $\log (S(t))_{p'} = (p'/p) \log (S(t))_p$, and was confirmed (empirically) by using normal equation analysis on two survival probability curves which had trap densities that bracketed the desired p value.[16] This calculation requires the construction of the *normal equations* for this system, which satisfy the relationship $A^T A\mathbf{x} = A^T\mathbf{b}$, where the resulting vector, $\hat{\mathbf{x}}$, is the least-squares solution to the system of equations $A\mathbf{x} = \mathbf{b}$. Here, the basis functions that are used to form A are the log $S(t)$ functions calculated for different trap concentrations and the fitted curve, $\mathbf{b}$ being the desired log $S(t)$ for some trap concentration within the range of trap concentrations used for the basis function curves. As can be seen in Figure 7, the exact, calculated curve and the interpolated curve are indistinguishable. This interpolation scheme would be expected to be very important in fitting experimental data to theoretical calculations.

When the theory behind this behavior is investigated, it is not surprising that the relationship appears exponential. Random-walk studies done by Zumofen and Blumen[17] indicate that at low trap concentrations ($p \leq$

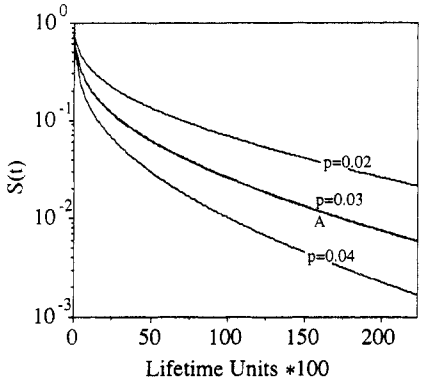

Figure 7. Calculated $S(t)$ curves for a polymer ensemble with an indicated trap density (ρ) and $\phi = 0.0$. The interpolated curve (A) for $r = 0.03$ overlays the exact curve with this trap density.

3%) the survival probability for 3-dimensional regular lattices is approximated very well by a single exponential whose argument is linear in p. The theoretical justification for this linearity follows from the description of the survival probability in terms of the probability that trapping has not occurred up to the nth step (F_n). If R_n represents the number of distinct sites visited in n steps, then

$$S(t=n\tau_0)_n = \langle F_n \rangle = \langle (1-p)^{R_n-1} \rangle = e^{\lambda} \langle e^{-\lambda R_n} \rangle \quad (13)$$

where τ_0 is the hopping time. This equation is then expanded in a cumulant expression, and the evaluation is truncated at the second cumulant

$$S(t)_2 = \exp(-\lambda X_n + \lambda^2 \sigma_n^2) \quad (14)$$

where $\lambda = -\ln(1-p)$ and X_n and σ_n^2 are the mean and the variance of R_n respectively. The log of the survival probability is thus $(-\lambda X_n + \lambda^2 \sigma_n^2)$, and at low trap concentration, $\lambda \approx -p$ and $\lambda^2 \approx 0$ (with less than 3% error for $p \leq 0.03$), thus making log $S(t)$ approximately linear in p.

(5) Calculation of Depolarization for Low Loading Polymers: Comparison to Experiment. Theoretical depolarization calculations were carried out on polymer ensembles for comparison with excitation transport theory predictions of data obtained for poly(2-ethylnaphthalene-*co*-methyl methacrylate) (2-EN-*co*-MMA) in a solid solution of PMMA. The initial parameters for these calculations as well as the corresponding results for $\langle R_g^2 \rangle^{1/2}$ and theoretical curves predicted by excitation transport theory were provided by Fayer.[9] Our depolarization calculations for polymer coils at $\phi = 0.275$ with a low chromophore loading are virtually indistinguishable from those calculated by Fayer and co-workers whose theory assumes that the polymer is a Gaussian coil. This is consistent with the finding that $\phi = 0.275$ corresponds to the Θ-point of the polymer. The agreement between curves for a sample having a degree of polymerization of 240 is shown in Figure 8, with the root-mean-square radius of gyration for the calculations listed in Table II. The calculated $\langle R_g^2 \rangle^{1/2}$ for 2-EN-*co*-MMA in a solid solution of PMMA compares well with that calculated by excitation transport theory[18] for every chromophore concentration and degree of polymerization considered. A comparison between the calculated $G^s(t)$ by excitation transport theory and that calculated by our model at various ϕ values for the same degree of polymerization is shown in Figure 9. As can be seen, the $G^s(t)$ from excitation transport theory corresponds to an interaction energy parameter of $\phi = 0.275$. This confirms that the depolarization experiments of Peterson et al. are consistent with a polymer coil that is at Θ-point conditions in the solid solution.

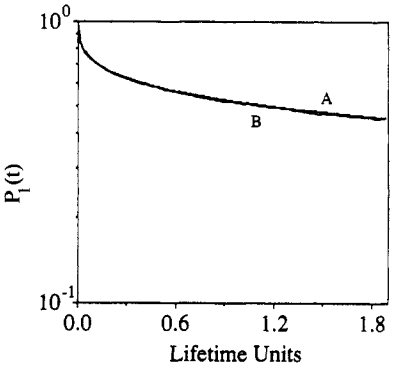

Figure 8. Depolarization (A) via EET vs calculated $G^s(t)$ (B) by excitation transport theory (see refs 5 and 19).

Table II
Length of Polymer Chain vs Root-Mean-Square Radius of Gyration

N	$\langle R_g^2 \rangle^{1/2\,a}$	$\langle R_g^2 \rangle^{1/2\,b}$
240	40	39.3
330	47	46.3
533	60	59.9
728	70	71.4

[a] Excitation transport theory[19] for 2-EN-*co*-MMA in a PMMA host. [b] Calculated for a sample of PMMA having a segment length 15.9 Å and a monomer length of 2.54 Å with $\phi = 0.275$.

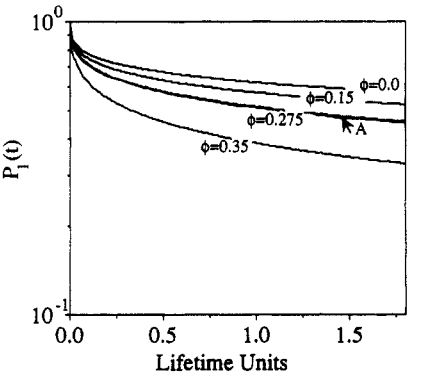

Figure 9. Depolarization curves, length = 533, 20 chromophores per coil. The curve predicted by excitation transport theory (A) is virtually identical to that calculated for $\phi = 0.275$ by our model.

The radius of gyration for a polymer is very dependent on the polymer length. In these calculations, we noticed that $\langle R_g^2 \rangle^{1/2}$ was so strongly dependent on the polymer length that a change in ϕ from 0 to 0.35 could not counteract a 30% increase in the polymer length. Thus it is essentially impossible to reproduce the correct $\langle R_g^2 \rangle^{1/2}$ and depolarization behavior by balancing errors in the choice of the polymer length and ϕ value. This implies that time-dependent fluorescence depolarization in trapped polymers represents a potentially powerful method for evaluating morphology–interaction parameter relations for a monodisperse polymer sample in the solid state.

Discussion

Long-range Förster type transfer is the accepted mechanism for energy migration along polymer coils that have chromophores with an allowed dipole transition. Since the underlying morphology of the coil directly affects the observed fluorescence properties of the system, we have attempted to provide a useful yet general model for EET and DEt on polymer coils. The major omission in our calculations is the time dependence of the rate matrix. Thus, our calculations are only applicable in those cases where the polymer coils are "frozen" or where the excited

state decays very rapidly with respect to polymer motion. In the case of coils with a low chromophore loading, the time dependence of the rate matrix is not as critical in the calculation of depolarization since the excitation is assumed to be depolarized after its first hop to another chromophore. This is an assumption which introduces little error, since the residual polarization for uncorrelated chromophores is approximately 4%. However, if rotational depolarization is much more facile than that due to DET, this method cannot be applied accurately.[18]

When transfer to non-nearest-neighbor chromophores is included in the calculation of the survival probability, the rate of transfer and trapping increases. We find that increasing the transfer radius from 1 to 3 lattice units incorporates approximately 99% of the total allowed transfer probability (see Figure 4). The convergence of the calculated survival probability with increasing allowed transfer distance is shown in Figure 3 and demonstrates that utilizing a 3 lattice unit cutoff for allowed transfer probability generates an accurate depiction of the true survival probability of the system and pemits utilization of the Lanczos algorithm for solving the rate equation.

There is a significant effect of the method of placing traps on the polymer chain. The long-time behavior of the different methods can be understood when the polymer morphology is considered. The excitation which typically hops from chromophore to chromophore along the polymer chain is frequently constrained to a small section of the coil by a "bottleneck" effect. This effect is observed whenever the excitation resides in a part of the polymer that contains no traps and can only interact with the remaining portion(s) of the polymer along a small number of pathways, each of which have a low probability of transfer. This effect is less pronounced for a random placement of traps, and the excitation is therefore trapped more uniformly and more rapidly.

The short-time behavior for the different trap placement methods is easily understood by realizing that traps placed on contact sites will trap excitation more rapidly because there are a large number of chromophores nearby. This effect was observed for every case investigated. This implies that the relationship between photophysics and polymer morphology will be different for the case of covalently bound traps, presumably placed at random positions along the chain, and self-trapping or quenching at excimer-forming sites. Polymers in which both phenomena occur (which is the usual case for photon-harvesting polymers) are expected to exhibit very complex behavior, based on our simulations.

While the linear dependence of log $S(t)$ on the trap density (p) at low trap densities has been investigated in other work,[17] we find that it is useful here in the generation of the survival probability curves for different values of p. This approximately linear interpolation method was found to work for any of the different trap placements investigated here. Furthermore, we have found that it is possible to accurately interpolate between different ϕ values for ensembles generated using the pivot algorithm. Thus it will be possible to map out the survival probability curves for a wide range of ϕ and p values.[19]

Acknowledgment. This work has been supported by the NSF Polymer Program (Grant DMR 9000562) and the State of Texas Advanced Research Program (Grant 4652). We thank Prof. M. D. Fayer, Department of Chemistry, Stanford University, Stanford, CA, for sending us his time-dependent depolarization data.

References and Notes

(1) *Photophysics of Polymers*; Hoyle, C. E., Torkelson, J. M., Eds.; ACS Monograph Series 358; American Chemical Society: Washington, DC, 1987.
(2) *Molecular Dynamics in Restricted Geometries*; Klafter, J., Drake, J. M., Eds.; John Wiley & Sons: New York, 1989.
(3) Byers, J. D.; Friedrichs, M. S.; Friesner, R. A.; Webber, S. E. *Macromolecules* **1988**, *21*, 3402.
(4) Byers, J. D.; Parsons, W. S.; Friesner, R. A.; Webber, S. E. *Macromolecules* **1990**, *23*, 4835.
(5) Peterson, K. A.; Fayer, M. D. *J. Chem. Phys.* **1986**, *85*, 4702.
(6) Förster, T. *Ann. Phys. (Leipzig)* **1948**, *2*, 55.
(7) Johnson, L. A.; Monge, A.; Friesner, R. A. *J. Chem. Phys.*, to be published.
(8) Some of the ensembles in our previous calculations provided to be statistically inaccurate when tested for convergence.
(9) Fayer, M. D. Private Communication. The development of the theory we label excitation transport theory herein is outlined in ref 18.
(10) Nadras, N.; Sokal, A. D. *J. Stat. Phys.* **1988**, *50*, 109.
(11) Bishop, M.; Clarke, J. H. R. *J. Chem. Phys.* **1991**, *94* (5), 3936.
(12) Friedrichs, M. S. Solution of the Pauli Master Equation for Disordered and Inhomogeneous Systems via the Lanczos Algorithm and Recursive Residue Generation Method. Ph.D. Dissertation, The University of Texas at Austin, 1987.
(13) Nauts, A.; Wyatt, R. E. *Phys. Rev. Lett.* **1983**, *51*, 2238.
(14) Friedrichs, M. S.; Friesner, R. A. *Chem. Phys. Lett.* **1987**, *137*, 285.
(15) Wilkinson, J. H.; Reinsch, C. *Linear Algebra, vol. II, of Handbook for Automatic Computation*; Springer-Verlag: New York, 1971.
(16) Leon, S. J. *Linear Algebra with Applications*; Macmillan: New York, 1980.
(17) Zumofen, G.; Blumen, A. *Chem. Phys. Lett.* **1982**, *88* (1), 63.
(18) Peterson, K. A.; Zimmut, M. B.; Linse, S.; Domingue, R. P.; Fayer, M. D. *Macromolecules* **1987**, *20*, 168.
(19) Byers, J. D. The Computer Simulation of Electronic Energy Transfer on Polymers in Solution. Ph.D. Dissertation, The University of Texas at Austin, 1992.